Crystal structure of phosphodiesterase 4D and inhibitor complex[1]

Mi Eun Lee[a], Joseph Markowitz[b], Jie-Oh Lee[a,*], Hayyoung Lee[c,*]

[a] *Department of Chemistry, Korea Advanced Institute of Science and Technology, 373-1 Kusong-dong, Yusong-gu, Daejon 305-701, South Korea*
[b] *Department of Biochemistry and Molecular Biology, University of Maryland School of Medicine, Baltimore, MD 21201, USA*
[c] *Institute of Biotechnology, Chungnam National University, Kung-dong, Yusong-gu, Daejon 305-764, South Korea*

Received 30 July 2002; accepted 19 August 2002

First published online 27 September 2002

Edited by Maurice Montal

Abstract **Cyclic nucleotide phosphodiesterases (PDEs) regulate physiological processes by degrading intracellular second messengers, adenosine-3′,5′-cyclic phosphate or guanosine-3′,5′-cyclic phosphate. The first crystal structure of PDE4D catalytic domain and a bound inhibitor, zardaverine, was determined. Zardaverine binds to a highly conserved pocket that includes the catalytic metal binding site. Zardaverine fills only a portion of the active site pocket. More selective PDE4 inhibitors including rolipram, cilomilast and roflumilast have additional functional groups that can utilize the remaining empty space for increased binding energy and selectivity. In the crystal structure, the catalytic domain of PDE4D possesses an extensive dimerization interface containing residues that are highly conserved in PDE1, 3, 4, 8 and 9. Mutations of R358D or D322R among these interface residues prohibit dimerization of the PDE4D catalytic domain in solution.**

Key words: Phosphodiesterase-4; Zardaverine; Rolipram; Cyclic adenosine-3′,5′-phosphate; X-ray crystal structure

1. Introduction

Changes in intracellular concentration of adenosine-3′,5′-cyclic phosphate (cAMP) or guanosine-3′,5′-cyclic phosphate (cGMP) mediate the action of numerous hormones and neurotransmitter signals important for cell growth, differentiation, survival, and inflammatory processes [1,2]. Phosphodiesterases (PDEs) are a divergent family of enzymes catalyzing the hydrolysis of these cyclic nucleotides and therefore provide the major pathway for eliminating the cyclic nucleotide signal from cells. Twelve different mammalian PDE families have been described, and these can be further divided into more than 50 subtypes and splice variants.

PDE families share the same general structure. A conserved region of approximately 380 amino acid residues in carboxy terminal half of the protein contains a catalytic domain that consists of 17 α-helices and a short β-hairpin [3]. This region is conserved between members of the same gene family. A binuclear metal center crucial for catalysis is located in a highly conserved pocket surrounded by helices H6, H13, and the loop between H7 and H8. Binding site of the adenine ring of the substrate is predicted in the adjacent hydrophobic pocket. However, the exact structure of substrate or substrate analog bound to the pocket has not been available yet.

The amino terminal half of PDE sequences contains highly variable domains that may be involved in enzyme regulation. Based on sequence homology, the PDE superfamily can be divided into two groups [1]. The first group is comprised of PDE2, 5, 6, 10 and 11. These PDE families contain one or two GAF domains in their amino terminal regions. PDE5, 6 are highly specific to cGMP and PDE2, 10 and 11 can hydrolyze both cAMP and cGMP. The second group includes PDE1, 3, 4, 7, 8 and 9. PDE families in this group lack GAF domains. Instead they have variable domains that are involved in enzyme regulation. In general, the second group of PDEs favors cAMP over cGMP for a substrate. PDE4, 7 and 8 are highly specific to cAMP and PDE1, 3 and 9 are dual specific enzymes.

Dialkoxyphenyl containing molecules have been shown to be selective inhibitors of PDE4 and are being developed as drugs against asthma and chronic obstructive pulmonary disease [4,5]. Zardaverine is a representative example of these inhibitors [6]. Although these drugs have been extensively studied, detailed structural information about enzyme and inhibitor interaction remains to be elucidated. In order to further understand the mechanism of the enzyme reaction and to facilitate the development of PDE inhibiting drugs, we undertook structural studies of the PDE4D catalytic domain and zardaverine complex.

2. Materials and methods

The minimal catalytic domain of PDE4D (residues 183T to 510S, GenBank IDU02882) was cloned into a GST fusion expression vector pGEX4T3 (APbiotech). The fresh transformation mixture was used directly for large-scale culture without colony purification. Due to the toxicity of the PDE gene, even a single round of colony purification eliminated soluble expression of the protein. Protein expression was induced at room temperature using 0.4 mM IPTG. After 12 h of the induction, the cells were harvested and lysed in a buffer containing 50 mM Tris, pH 8.0, 0.4 M NaCl, 5 mM DTT by sonication after 0.2 mg/ml lysozyme treatment on ice. The cell lysate was centrifuged and the supernatant was loaded on a Q-Sepharose (APbiotech) ion exchange column pre-equilibrated with the lysis buffer. The flow-through fractions were collected and loaded on a glutathione–Sepharose column (APbiotech). The bound protein was eluted with a buffer containing 5 mM glutathione, 50 mM Tris, pH 8.0, 0.4 M NaCl, 5 mM DTT. The GST–PDE4D fusion protein was cleaved by 0.5% (w/w protein) thrombin at 4°C overnight. PDE4D was further purified by

*Corresponding author. Faxes: (82)-42-869 5839, (82)-42-822 9690.
E-mail addresses: jieoh@kaist.ac.kr (J.-O. Lee), hlee@cnu.ac.kr (H. Lee).

[1] Atomic coordinates (code 1MKD) have been deposited in the Protein Data Bank.

Abbreviations: PDE, phosphodiesterase; cAMP, adenosine-3′,5′-cyclic phosphate; cGMP, guanosine-3′,5′-cyclic phosphate; NCS, non-crystallographic symmetry

0014-5793/02/$22.00 © 2002 Published by Elsevier Science B.V. on behalf of the Federation of European Biochemical Societies.
PII: S0014-5793(02)03396-3

Source Q anion exchange and Superdex-200 gel filtration chromatography (APbiotech). The purified protein was concentrated to 70 mg/ml and used for crystallization. Catalytic activity of the purified protein was confirmed as previously described [7,8].

PDE4D–zardaverine complex was crystallized using hanging drop vapor-diffusion. The concentrated protein solution was mixed with zardaverine solution at a final concentration of 3 mM. After 10 min incubation at 4°C, the protein–inhibitor complex was crystallized by mixing 2 μl protein and 2 μl crystallization solution containing 0.1 M sodium cacodylate, pH 6.5, 11% PEG 8000, 0.6 M magnesium acetate, and 5 mM DTT at room temperature. Protein crystals with a typical size of 50×50×100 μm were grown after 1 week. Well isolated single crystals were separated from large crystal clusters and frozen in a buffer containing 30% ethylene glycol, 0.1 M sodium cacodylate, pH 6.5, 11% PEG 8000, 0.6 M magnesium acetate, and 5 mM DTT using a stream of boiling liquid nitrogen. A complete data set to 2.9 Å was collected at the A1 beam line in the Cornell High Energy Synchrotron Source. The data were indexed with DENZO, and scaled and reduced with SCALEPACK [9].

The PDE4D–zardaverine structure was solved by molecular replacement using the structure of PDE4B catalytic domain as a search probe. The molecular replacement calculations were performed with the program AmoRe [10]. The structure was refined using program CNS [11] with 95% of the data. Five percent of the data was reserved for the R_{free} calculation. Positions of the atoms related by non-crystallographic symmetry (NCS) were tightly restrained throughout the refinement. The R factor dropped from 48% to 27% in a single round of automatic refinement. A strong and continuous electron density near the metal binding sites was found after 12-fold NCS averaging (Fig. 1C). Twenty low energy conformations of zardaverine generated from conformational analysis using a program Cache (Fujitsu) were fitted to the density. The best conformation of zardaverine was obvious and selected for the final refinement. The final model contains 12 PDE4D catalytic domains. Each protein includes one zinc, one magnesium, one dimethylarsenate (cacodylate), and one zardaverine molecule.

3. Results and discussion

3.1. Overall structure

The minimal PDE4D catalytic domain [12] was crystallized in the presence of 3 mM zardaverine. The structure of the protein–inhibitor complex was determined by molecular replacement using the inhibitor-free PDE4B structure as a

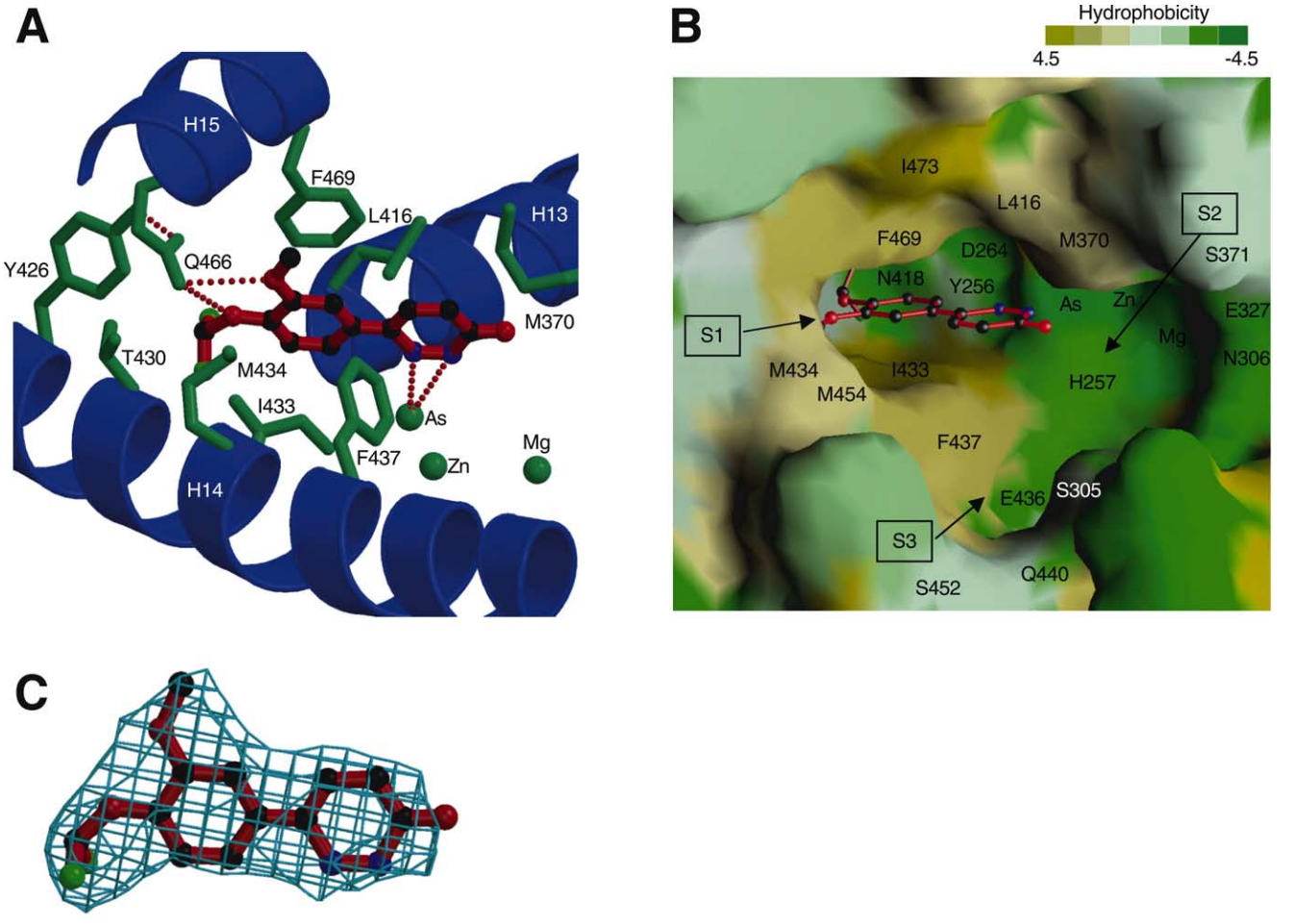

Fig. 1. The structure of zardaverine bound to the PDE4D active site pocket. A: Protein residues are shown in green. Helices are drawn schematically as blue ribbons. The helix-numbering scheme of PDE4D is identical with that of PDE4B [3]. Carbon, nitrogen, oxygen and fluorine atoms in zardaverine are shown in black, blue, red, and green respectively. Potential hydrogen bonds are drawn in broken red lines. 'As' represents the dimethylarsenate ion. B: Surface representation of the active site pocket. Bound zardaverine is shown using a ball-and-stick model. The hydrophobic and hydrophilic surfaces of the protein are colored in yellow and green, respectively. Kyte and Doolittle's hydrophobicity scale was used for the calculation [22]. The positions of S1, S2, and S3 sub-pockets are indicated by arrows. The residues important for inhibitor binding are written on the surface. P419 is located under F469 and not visible in this orientation. W429 is hidden behind the difluoromethoxy group of zardaverine. C: Twelve-fold NCS averaged 2Fo–Fc electron density map calculated with a model without bound zardaverine. The refined atomic model of zardaverine is superimposed.

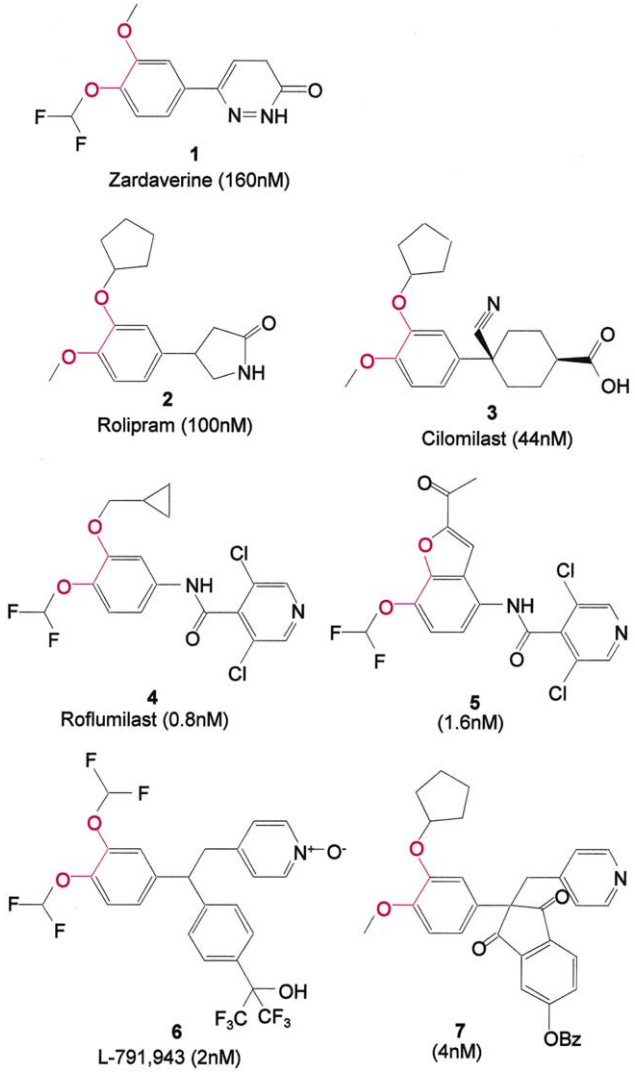

Fig. 2. Dialkoxyphenyl containing PDE4 inhibitors [4,6,15,16,23–25]. IC_{50} values are written in parentheses. The dialkoxy pharmacophores are colored in red.

search probe (Table 1). The PDE4D catalytic domain has 16 α-helices from H1 to H16 and a short β-hairpin. Helices H0 and H17 are not essential for the catalytic activity and were deleted in the crystallized catalytic domain. The active site pocket of PDE4D includes both the inhibitor and metal binding sites. The binuclear metal binding site, important for catalysis, is surrounded by helices H6, H13, and the loop between H7 and H8. Zardaverine binds to mostly hydrophobic part of the active site pocket (Fig. 1). Zardaverine binding induces few structural changes in the protein, except for minor rearrangements of the side chains. The metal coordination geometry exhibits few changes and the arsenate ion mimicking catalytic phosphoryl group is also conserved in the zardaverine bound PDE4D structure.

3.2. Structural comparison of PDE4D and PDE4B catalytic domains

Amino acid sequences of the catalytic domains of PDE4D and PDE4B are highly conserved (80% identity) and their structures can easily be superimposed. Especially residues located near the metal and inhibitor binding sites are completely conserved. Most of the unconserved residues are concentrated in the helices H2, H3, H5 and intervening loops. However, even these most divergent regions show only trivial structural deviations. Furthermore, these regions are located away from the enzyme active site and thus unlikely play direct roles in the catalysis.

3.3. Structure of the inhibitor binding pocket

The zardaverine pocket is approximately 12 Å deep and has an elongated opening 20 Å long by 4.5 Å wide. The shape of the pocket complements planar and extended PDE inhibitors and substrates [4]. The upper and lower walls of the binding pocket are rimmed by hydrophobic residues, F469, L416, M370, M434, I433, F437, and M454 (Fig. 1A,B). In particular, the phenolic ring of zardaverine is parallel to F469 with inter-planar distance of 3.2 Å. F469 is invariant in known PDE families and the mutation of F469 in PDE4A has enzymatic activity and inhibitor binding decreased by more than a 100-fold [12]. Mutations of I433, F437 and M434 also have greatly reduced inhibitor binding [13]. Potential hydrogen bonding partners are located in the back and left side of the pocket. Of these residues, Q466 and Y256 are highly conserved in PDE families. However, residues N418, P419, Y426, D264 and T430 of PDE4D have significant sequence variations and may provide substrate and inhibitor selectivity of the enzyme [14]. Zardaverine is a specific inhibitor of PDE3 and PDE4 [6]. Its selectivity is provided, in part, by two hydrogen bonds. Ether oxygens of the dialkoxy pharmacophore make strong hydrogen bonds to the amide nitrogen of the Q466 side chain. The difluoromethoxy group of zardaverine occupies a small sub-pocket surrounded by N418, T430, P419, Y256, and W429. The structure of the fluorine sub-pocket is rigid and too small to accept bigger chemical groups. The substitution of difluoromethoxyl by bulkier functional groups significantly reduces the inhibitors' binding affinity to the pro-

Table 1
Data collection and refinement statistics

Space group	$P2_12_12_1$
Cell dimensions (Å)	$a = 97.3$, $b = 164.6$, $c = 325.5$
Resolution (Å)	20.0–2.9
Total reflections	730 381
Unique reflections	114 897
Completeness (%)	99.3 (99.2)[a]
R_{merge} (%)[b]	7.3 (36.7)[a]
Resolution (Å)	20.0–2.9
Number of protein molecules in asymmetric unit	12
Reflections	114 897
R_{free} (%)[c] ($\|F\| > 0\ \sigma$)	27.1
R_{cryst} (%)[c] ($\|F\| > 0\ \sigma$)	22.9
Average *B*-value	
Protein	46.4
Ligand	56.1
R.m.s deviations from ideality	
Bonds (Å)	0.008
Angles (°)	1.26
Improper angles (°)	0.82

[a] Statistics of the highest resolution shell are shown in parentheses.
[b] $R_{merge} = \Sigma_{hkl}\Sigma_j |I_j(hkl) - \langle I(hkl)\rangle| / \Sigma_{hkl}\Sigma_j |I_j(hkl)|$, where $I_j(hkl)$ and $\langle I(hkl)\rangle$ are the intensity of measurement j and the mean intensity for the reflection with indices hkl, respectively.
[c] $R_{cryst,free} = \Sigma_{hkl} \| F_{calc}(hkl)| - |F_{obs}(hkl) \| / \Sigma_{hkl} |F_{obs}|$, where the crystallographic and free *R*-factors are calculated, including and excluding refined reflections, respectively. The free reflections constituted 5% of the total number of reflections.

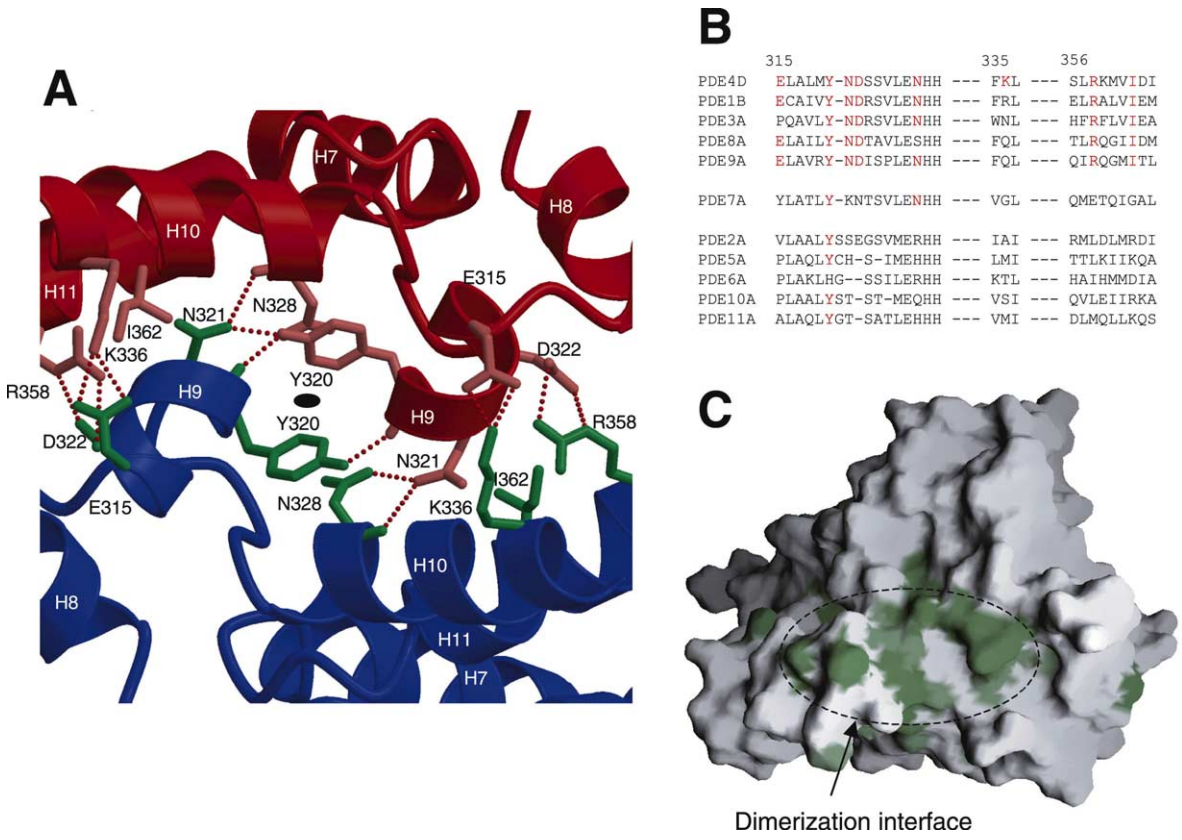

Fig. 3. The structure and conservation of the dimerization interface. A: The two subunits of PDE dimer are shown in red and blue. The position of a non-crystallographic two-fold axis is marked by a filled ellipsoid. Important interface residues are drawn. Potential hydrogen bonds are shown in broken red lines. B: Sequence alignment of interface residues. Representative members of each PDE family are aligned. Conserved interface residues are shown in red. C: Surface representation of PDE4D catalytic domain. Surface area conserved more than 80% is colored in green. Amino acid sequences of PDE1, 3, 4, 8 and 9 were aligned for calculation of conservation.

tein [15]. Interestingly, the fluorine sub-pocket has two potential hydrogen bond acceptors, N418 Oδ and T430 Oγ. Therefore, replacing hydrogen accepting fluorine atoms with hydrogen donating groups may greatly improve the inhibitor's potency and selectivity. Two nitrogen atoms in the pyridazinone ring are situated at a distance that is ideal for hydrogen bonding from the arsenate binding site [3]. In physiological conditions, the arsenate site is probably occupied by phosphate ions. Most of the PDE4 selective inhibitors contain hydrogen donors or acceptors at similar positions that may interact with the arsenate oxygens (Fig. 2) [4].

Zardaverine fills approximately half of the active site pocket. Recently developed and more selective PDE4 inhibitors are likely to utilize empty sub-pockets for additional binding energy and selectivity [4]. For clarity of description, we call these sub-pockets S1, S2, and S3 (Fig. 1B). Structural comparison of dialkoxy containing PDE inhibitors is relatively straightforward, due to the elongated planar shape of the molecule and common dialkoxy pharmacophore (Fig. 2). The S1 sub-pocket, formed by M434, M454, and F437, is a shallow groove rather than a deep pocket. In the inhibitors more specific than zardaverine, the methoxy group of dialkoxy pharmacophore is replaced by bulkier groups that may pack against the S1 surface. Rolipram and cilomilast have cyclopentyl groups while roflumilast contains a cyclopropyl group. The 7-methoxybenzofuran derivative (compound 5, Fig. 2) has an acetylfuran ring replacing the methoxy group of the dialkoxy pharmacophore in zardaverine.

The S2 sub-pocket consists of side chains of M370, S371, E327, N306, D369, metal ions and the arsenate ion (Fig. 1B). Specific PDE4 inhibitors tend to have more elongated structures than zardaverine, capable of filling the S2 sub-pocket. Roflumilast has an additional amide group and the inhibitor L-791,943 has two extra carbons in its chemical backbone. The extended chemical chains may interact more efficiently with the hydrophobic wall made of M370, explaining the higher affinity and selectivity of these inhibitors. Even these selective compounds do not completely fill the S2 sub-pocket of PDE4D. Sufficient space remains for a few more carbon chains. If additional carbon chains and hydrogen-bonding partners could be designed in the S2 sub-pocket, then the potency and selectivity of the compound might be improved.

The S3 sub-pocket branches approximately 90° from the middle of the main active site pocket. Residues F437, E436, Q440, S305, C455, and S452 line the wall of the S3 sub-pocket. The additional aromatic rings of L-791,943 and the indan-1,3-dione derivative (compound 7, Fig. 2) could occupy the S3 pocket and make hydrophobic and hydrogen bonding interactions with the protein side chains. A previous modeling study with L-791,943 and the indan-1,3-dione derivative demonstrated that the additional aromatic rings branch perpen-

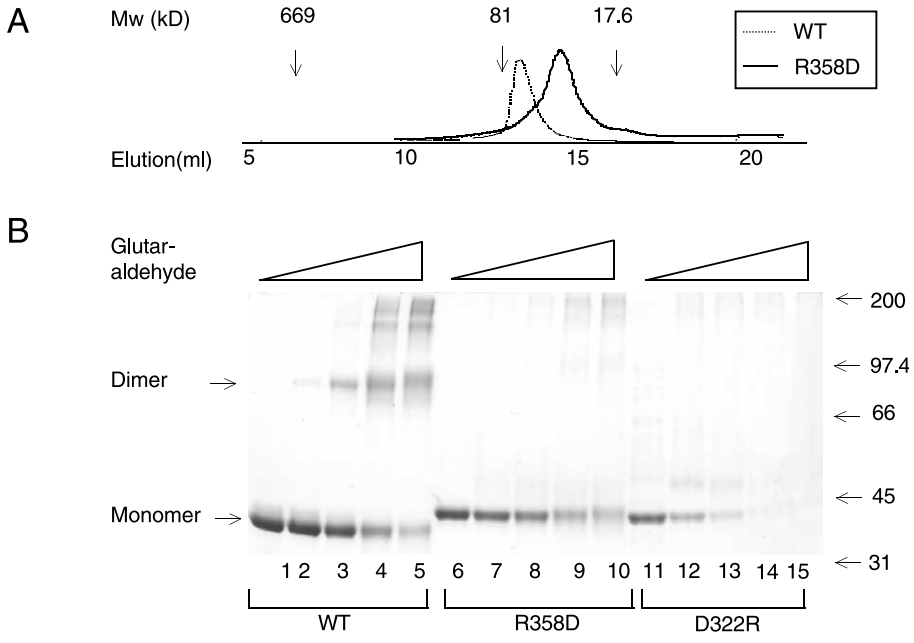

Fig. 4. The dimerization of wild type and mutant PDE4D catalytic domain. A: Purified wild type and R358D mutant protein were injected into a Superdex 200 (APbiotech) gel filtration column. Elution volumes for molecular weight standards are indicated. B: Glutaraldehyde-mediated cross-linking of the purified wild type and mutant proteins was performed as published [26]. The cross-linked proteins were separated by SDS–PAGE and stained with Coomassie brilliant blue R-250. Glutaraldehyde concentrations used for each lanes are, 1, 6, 11: 0%; 2, 7, 12: 0.01%; 3, 8, 13: 0.03%; 4, 9, 14: 0.1%; 5, 10, 15: 0.3%. Mutant catalytic domains of PDE4D were cloned into the pAcHLTA vector (BD Pharmingen) and expressed using a baculovirus expression system. Mutant proteins could not be overexpressed in *Escherichia coli*. They run in as slightly higher molecular weight due to hexa-histidine tags. In control experiments with wild type protein expressed in insect cells, the histidine tag did not affect cross-linking results (data not shown).

dicularly from the main ring systems [16]. The shapes of these molecules match well with the T-shaped PDE active site pocket. The S1, S2, and S3 sub-pockets are highly conserved overall, but they have variable patches. M434 and M454 of S1, M370 of S2 and S305, C455 and S452 of the S3 sub-pocket have significant sequence variations in known PDE families. These variable patches may provide good targets for the design of selective PDE inhibitors.

3.4. Arsenate binding site

The structure of zardaverine bound PDE4D exhibits a metal coordination geometry practically identical to that of ligand free PDE4B (Fig. 1A) [3]. The permanent metal ion, presumably zinc, is coordinated by H261, H297, D298, D415, and a bridging hydroxide ion. The variable metal ion that is likely to be magnesium from the crystallization buffer is coordinated by D298, the shared bridging hydroxide, and four water molecules. In PDE4B structure, Xu et al. found an arsenate binding site located 2.6 Å from the site of the metal center. This arsenate site is also conserved in the zardaverine bound PDE4D structure. In our zardaverine bound PDE4 structure, the arsenate site is occupied by dimethyl arsenate (cacodylate) from the crystallization buffer. The observation that both PDE4B and PDE4D, crystallized in very different conditions, contain anion binding sites at the same positions strongly supports the hypothesis that the arsenate may mimic the phosphoryl ester in cyclic nucleotide substrates. Furthermore, the position and geometry of the PDE arsenate site is similar to those of the substrate mimicking tungstate site in protein phosphatase I [17]. Protein phosphatase I also contains a binuclear metal center in the active site and has a reaction mechanism similar to that of PDE.

3.5. Dimerization of PDE

PDE4D–zardaverine complex forms a dodecamer in the asymmetric unit of the crystal. Dimers of PDE trimerize to form a hexameric unit. The two hexameric units stack in a tail-to-tail manner and become a dodecameric complex in the crystal. Trimeric and hexameric interfaces are unlikely to have biological significance because their contact areas are limited and the mediating residues are highly variable in known PDE sequences. On the other hand, the dimeric interface could represent a physiological dimer interface (Fig. 3A). Both full length and the catalytic domain of PDE4 multimerize in solution (Fig. 4) [18]. To verify that this crystallographic dimer interface is part of the multimerization interface in solution, either R358D or D322R mutation was introduced to the PDE4D catalytic domain. These residues were chosen because they do not have structural roles other than dimerization. The electrical charge of the residues was reversed to disrupt dimer interactions efficiently. The oligomeric state of the purified mutants was probed by glutaraldehyde-mediated cross-linking (Fig. 4B). In the condition where the wild type protein was cross-linked as a dimer, neither of the mutant proteins was cross-linked. Furthermore, the purified R358D mutant protein was eluted later than wild type protein in gel filtration chromatography, which is consistent with the monomeric state of the mutant and dimeric state of the wild type protein (Fig. 4A). These data confirm that the crystallographic dimer interface indeed mediates protein dimerization in solution. Residues involved in the dimerization, E315, N321, D322, N328, R358, and I362, are highly conserved in PDE1, 3, 4, 8, and 9 but not in PDE2, 5, 6, 7, 10, and 11 (Fig. 3B). Consistent with the sequence homology data, the catalytic domain of PDE5 has been shown to be a monomer in solution [19]. Interest-

ingly, PDE2, 5, 6, 10 and 11 are closely related to each other in evolution and contain GAF domains in their amino terminal region [1,2,20,21]. PDE7 is the only exception. Although PDE7 does not contain GAF domains, its amino acid sequences are closely related to the GAF containing PDEs in the phylogenetic tree [1,21]. In the PDE4 catalytic domain, the dimer interface is the most conserved surface besides the active site pocket (Fig. 3C). High sequence conservation of the interface residues in PDE1, 3, 4, 8, and 9 suggests that dimerization mediates indispensable biological functions for these types of PDEs including PDE4D.

3.6. Conclusions and implications

This is the first structure of PDE–inhibitor or PDE–substrate analog complex. Majority of PDE4 specific inhibitors under development contain dialkoxyphenyl pharmacophore [4]. Our zardaverine–PDE4D structure shows how these inhibitors interact with the enzyme. It also provides clues about PDE and substrate interactions and illustrates the structure of the evolutionary conserved dimerization interface. This structure will be used as a template for the design of novel PDE inhibiting drugs.

Acknowledgements: We thank the staff of the Cornell High Energy Synchrotron Source (MacChess) for help with data collection. This study was supported by a grant of the Korea Health 21 R&D Project, Ministry of Health and Welfare, Republic of Korea (01-PJ1-PG3-20900-0029) and funds from University of Maryland Baltimore County. J.M. is supported by the MD/PhD program of the University of Maryland School of Medicine. Part of the research was done while J.-O.L and H.L. were in University of Maryland at Baltimore County.

References

[1] Francis, S.H., Turko, I.V. and Corbin, J.D. (2001) Prog. Nucleic Acid Res. Mol. Biol. 65, 1–52.
[2] Houslay, M.D. (2001) Prog. Nucleic Acid Res. Mol. Biol. 69, 249–315.
[3] Xu, R.X. et al. (2000) Science 288, 1822–1825.
[4] Huang, Z., Ducharme, Y., Macdonald, D. and Robichaud, A. (2001) Curr. Opin. Chem. Biol. 5, 432–438.
[5] Torphy, T.J. and Page, C. (2000) Trends Pharmacol. Sci. 21, 157–159.
[6] Schudt, C., Winder, S., Muller, B. and Ukena, D. (1991) Biochem. Pharmacol. 42, 153–162.
[7] Ball, E.H., Narindrasorasak, S. and Sanwal, B.D. (1979) Can. J. Biochem. 57, 1220–1228.
[8] Laiberte, F. et al. (2000) Biochemistry 39, 6449–6458.
[9] Otwinowski, Z. and Minor, W. (1997) Methods Enzymol. 276, 461–472.
[10] Navaza, J. (1994) Acta Crytallogr. A50, 157–163.
[11] Brunger, A.T. et al. (1998) Acta Cryst. D54, 905–921.
[12] Richter, W., Unciuleac, L., Hermsdorf, T., Kronbach, T. and Dettmer, D. (2001) Cell Signal. 13, 287–297.
[13] Atienza, J.M., Susanto, D., Huang, C., McCarty, A.S. and Colicelli, J. (1999) J. Biol. Chem. 274, 4839–4847.
[14] Herman, S.B., Juilfs, D.M., Fauman, E.B., Juneau, P. and Menetski, P. (2000) Mol. Pharmacol. 57, 991–999.
[15] Marivet, M.C. et al. (1989) J. Med. Chem. 32, 1450–1457.
[16] He, W. et al. (1998) J. Med. Chem. 41, 4216–4223.
[17] Egloff, M.P., Cohen, P.T., Reinemer, P. and Barford, D. (1995) J. Mol. Biol. 254, 942–959.
[18] Conti, M. et al. (1995) Biochemistry 34, 7979–7987.
[19] Fink, T.L., Francis, S.H., Beasley, A., Grimes, K.A. and Corbin, J.D. (1999) J. Biol. Chem. 274, 34613–34620.
[20] Fawcett, L. et al. (2000) Proc. Natl. Acad. Sci. USA 97, 3702–3707.
[21] Koyanagi, M. et al. (1998) FEBS Lett. 436, 323–328.
[22] Kyte, J. and Doolittle, R.F. (1982) J. Mol. Biol. 157, 105–132.
[23] Christensen, S.B. et al. (1998) J. Med. Chem. 41, 821–835.
[24] Ashton, M.J. et al. (1994) J. Med. Chem. 37, 1696–1703.
[25] McGarry, D.G. et al. (1999) Bioorg. Med. Chem. 7, 1131–1139.
[26] Pavletich, N.P., Chambers, K.A. and Pabo, C.O. (1993) Genes Dev. 7, 2556–2564.